

Longitudinal structure function F_L at low Q^2 and low x with model for higher twist: an update

Barbara Badełek¹ and Anna M. Staśto²

¹*Faculty of Physics, University of Warsaw, 02-093 Warsaw, Poland*

²*Department of Physics, Penn State University, University Park, PA 16802, USA*

February 10, 2022

Abstract

A reanalysis of the model for the longitudinal structure function $F_L(x, Q^2)$ at low x and low Q^2 was undertaken, in view of the advent of the EIC. The model is based on the photon-gluon fusion mechanism suitably extrapolated to the region of low Q^2 . It includes the kinematic constraint $F_L \sim Q^4$ as $Q^2 \rightarrow 0$ and higher twist contribution which vanishes as $Q^2 \rightarrow \infty$. Revised model was critically updated and compared to the presently available data.

1 Introduction

Knowledge of both F_2 and F_L structure functions, from the photoproduction to the deep inelastic region is needed in the calculations of QED radiative corrections to the data from the Deep Inelastic Scattering (DIS) process, $l+p \rightarrow l'+X$ (l, l' are leptons), Ref. [1]. This knowledge is also essential in verifying the sum rules, e.g. the Gottfried sum rule or (in case of the spin-dependent function g_1) the Bjorken sum rule [2], a fundamental relation of Quantum ChromoDynamics (QCD). Thus the electroproduction structure functions, F_2 , F_L and g_1 in the full kinematic region are indispensable in the data analysis, especially in the context of the future DIS facilities like the Electron Ion Collider (EIC), currently planned in the US [3]. In this paper we shall consider the spin-independent longitudinal structure function F_L .

The structure functions depend on two variables: x and Q^2 , conventionally defined as $x = Q^2/(2p \cdot q)$ and $Q^2 = -q^2$ where q and p denote the four momentum transfer between

the incident and scattered leptons and the four momentum of the target proton respectively; these four-vectors and the four-momentum p_l of the incident lepton, define the inelasticity y as $y = p_l \cdot p / (q \cdot p)$. Unlike F_2 and g_1 , the experimental data for F_L are rather scarce for the low Q^2 values and thus an extrapolation to this region needs to be performed with a physically motivated model with least number of free parameters. The model should also contain an extrapolation to the region of low x , as data both from fixed-target and colliders correlate these two kinematic regions. Such model for F_L was proposed some time ago [4]. It was based on the k_T -factorization formula which involves the unintegrated gluon density with their transverse momentum (k_T) dependence. The k_T -factorization was derived in the high-energy limit of $s \gg |t|$, where s is the centre-of-mass energy squared in the scattering process and t is the four-momentum transfer in the t -channel. It was derived for processes like heavy quark production in hadron-hadron collisions as well as for DIS. In principle the unintegrated gluon distribution should be obtained from the Balitsky-Fadin-Kuraev-Lipatov (BFKL) equation, which resums the large logarithms of energy (or small x). In the model used in Ref. [4] the unintegrated gluon distribution function was constructed from the collinear integrated gluon density through the logarithmic derivative over the scale dependence. This effectively neglected higher order small x contributions in the gluon anomalous dimension; these contributions are expected to be significant only at extremely low values of x .

The k_T -factorization formula was then extrapolated to the low Q^2 region by introducing the cutoff on the low quark transverse momenta. This region is dominated by the soft physics with a higher twist contribution to F_L vanishing at large Q^2 . In the model it was treated phenomenologically and its normalization was determined from the (non-perturbative) part of the structure function F_2 . The model embodied the kinematic constraint $F_L \sim Q^4$ in the limit $Q^2 \rightarrow 0$ for fixed $2p \cdot q$. It thus contained only physically motivated parameters.

In this paper we revisit the model of Ref. [4] for the extrapolation of $F_L(x, Q^2)$ to the region of low values of Q^2 at low x . We have included the updated parametrizations of the Parton Distribution Functions (PDFs) for the quark and gluon densities in the proton, checked the sensitivity of the results to the assumed quark masses and tested the gluon distributions supplemented with the Sudakov form-factor.

The calculations have been compared with high Q^2 measurements of F_L by HERA and with low Q^2 data by SLAC and JLab. Here one has to be aware that most of the SLAC and JLab data are in the regime which only marginally overlaps with the region of applicability of the model, as they correspond to rather high values of $x \gtrsim 0.1$.

The outline of the paper is as follows. In the next section we discuss the general properties of the longitudinal structure function, in Sec. 3 the k_T -factorization is introduced, while in

Sec. 4 the details of the model for the higher twist are given. Numerical results are presented in Sec. 5. Finally, in Sec. 6 we state our conclusions.

2 Longitudinal structure function F_L

The longitudinal structure function $F_L(x, Q^2)$ corresponds to the interaction of the longitudinally polarized virtual photon in the deep inelastic lepton-nucleon scattering. In the low x region it is dominated by the gluon density. The experimental determination of F_L is rather challenging since it requires a measurement of the dependence of the DIS cross-section on y , for fixed values of x and Q^2 . This in turn requires performing measurements at varying centre-of-mass energies, see e.g. Ref. [5]. Unlike the F_2 structure function, where the experimental data are abundant, the number of F_L data points is rather limited so far and measurement errors are rather large.

In the ‘naive’ quark-parton model the structure function $F_L(x, Q^2)$ vanishes, as a consequence of quarks having spin 1/2. More precisely, F_L vanishes when the transverse momenta of the quarks are limited. At large Q^2 , F_L is proportional to $(\langle m_q^2 \rangle + \langle \kappa_T^2 \rangle)/Q^2$, where m_q is the quark mass and κ_T , the quark transverse momentum, is by definition limited in the naive parton model. This remains approximately valid in the leading logarithmic order in the collinear approximation. At higher logarithmic orders the point-like QCD interactions (gluon emissions) allow for the average transverse momenta $\langle \kappa_T \rangle$ to grow with increasing Q^2 . Thus at higher orders of perturbation theory $F_L(x, Q^2)$ acquires a leading twist contribution. In the limit of small x , the longitudinal structure function is driven by the gluons through the $g \rightarrow q\bar{q}$ transition and thus permits a direct measurement of the gluon density in the nucleon.

In the limit $Q^2 \rightarrow 0$ the structure function F_L has to vanish as Q^4 (for fixed $2p \cdot q$) which eliminates potential singularities at $Q^2 = 0$ of the hadronic tensor $W^{\mu\nu}$. It also reflects the vanishing of the cross section $\sigma_L \sim F_L/Q^2$ in the real photoproduction limit.

The longitudinal structure function is theoretically fairly well understood at high Q^2 , thanks to the framework of perturbative QCD. On the contrary, very little is known about its extrapolation towards the region of low Q^2 ; it is possible that it contains large contributions from higher twists there.

3 The k_T factorization

Structure functions in the limit of small x and at large Q^2 can be evaluated using the k_T -factorization theorem [6–12]. The basic process which we consider is photon - gluon fusion, $\gamma^* + g \rightarrow q + \bar{q}$, and the corresponding diagram in the lowest order of perturbation theory is shown in Fig. 1. The distinctive feature of the k_T -factorization formula is the fact that the gluon transverse momentum, here k_T , is taken into account, unlike in the collinear factorization framework, where the integrated parton density depends only on the fraction of the longitudinal nucleon momentum and the scale.

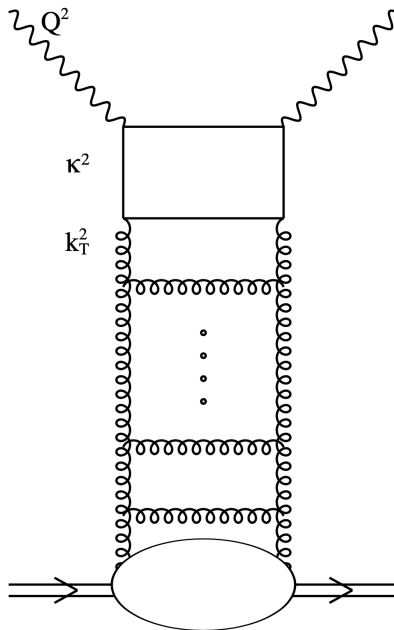


Figure 1: Diagrammatic representation of the photon-gluon fusion mechanism and of the k_T -factorization formula. Symbols κ^2 and k_T^2 denote the transverse quark momentum squared and gluon transverse momentum squared, respectively.

The photon-gluon fusion off-shell amplitude is known up to NLO accuracy [13–15]. In our model, we use the LO expression for that amplitude but with the additional corrections stemming from the exact kinematics, which effectively takes into account a part of the important higher order corrections [16, 17].

The expression for the longitudinal structure function can be written in the following

form

$$F_L(x, Q^2) = 2 \frac{Q^4}{\pi^2} \sum_q e_q^2 I_q(x, Q^2), \quad (1)$$

where I_q is defined by

$$I_q(x, Q^2) = \int \frac{dk_T^2}{k_T^4} \int_0^1 d\beta \int d^2\boldsymbol{\kappa}'_T \alpha_s \beta^2 (1-\beta)^2 \frac{1}{2} \left(\frac{1}{D_{1q}} - \frac{1}{D_{2q}} \right)^2 f(x_g, \mathbf{k}_T^2). \quad (2)$$

The denominators D_{1q}, D_{2q} are defined as

$$D_{1q} = \kappa_T^2 + \beta(1-\beta)Q^2 + m_q^2,$$

$$D_{2q} = (\boldsymbol{\kappa}_T - \mathbf{k}_T)^2 + \beta(1-\beta)Q^2 + m_q^2. \quad (3)$$

In Eq. (1) the sum runs over all the active quark flavours q , here u, d, s, c. The α_s is the strong coupling. The transverse momenta of the quark and gluon are denoted by $\boldsymbol{\kappa}_T$ and \mathbf{k}_T respectively, see Fig. 1. Let us define the shifted transverse momentum $\boldsymbol{\kappa}'_T$ as follows

$$\boldsymbol{\kappa}'_T = \boldsymbol{\kappa}_T - (1-\beta)\mathbf{k}_T. \quad (4)$$

The variable x_g is the fraction of the longitudinal momentum of the proton carried by the gluon which can be computed by taking into account the exact kinematics [18]

$$x_g = x \left(1 + \kappa_T'^2 + \frac{m_q^2}{\beta(1-\beta)Q^2} + \frac{k_T^2}{Q^2} \right). \quad (5)$$

The variable β is the corresponding Sudakov parameter appearing in the quark momentum decomposition into the basic light-like four vectors, p' and q' which are defined as

$$p' = p - \frac{M^2 x}{Q^2} q, \quad q' = q + xp, \quad (6)$$

where M is the target nucleon mass. We decompose four-vector κ as

$$\kappa = x_q p' - \beta q' + \boldsymbol{\kappa}_T, \quad (7)$$

where

$$x_q = x \left(1 + \frac{m_q^2 + \kappa_T^2}{(1-\beta)Q^2} \right). \quad (8)$$

The variable x_g in (5) is the fraction of the longitudinal momentum of the proton carried by the gluon, which couples to the quarks in the ‘quark-box’, see Fig.1. In the leading order

case this variable should be equal to Bjorken x . This is also the case in the dipole model formulation of the high energy scattering. Here however we include the exact kinematics, which effectively makes this fraction larger than x . This has significant numerical effects, as demonstrated for example in Ref. [19].

The unintegrated gluon density $f(x_g, k_T^2)$ should in principle be obtained from an equation which resums small x contributions, that is the BFKL equation. In Ref. [4] we used the approach where the unintegrated gluon density was computed from the standard integrated density by taking a logarithmic derivative

$$f(y, k_T^2) = y \frac{\partial g^{AP}(y, Q^2)}{\partial \ln Q^2} \Big|_{Q^2=k_T^2}, \quad (9)$$

where $g^{AP}(y, Q^2)$ satisfies the conventional (LO or NLO) DGLAP equations. In this approximation one neglects the higher order small x resummation effects in the gluon density and therefore in the gluon anomalous dimension. This approximation will be used in the present update of the model¹. We shall also use the gluon density from the Kimber-Martin-Ryskin approach [20, 21] which supplements the formula (9) with the Sudakov form-factor

$$f(y, k_T^2) = y \frac{\partial \left(g^{AP}(y, Q^2) T(Q, k_T) \right)}{\partial \ln Q^2} \Big|_{Q^2=k_T^2}, \quad (10)$$

defined as

$$T(Q, k_T) = \exp \left\{ - \int_{k_T^2}^{Q^2} \frac{dp_T^2}{p_T^2} \int_0^{1-\Delta} dz z P_{gg}(z, p_T) \right\}, \quad (11)$$

with the P_{gg} the gluon-gluon DGLAP splitting functions. The cut-off Δ is necessary to regulate the divergence at $z = 1$. As discussed in Ref. [22], different forms of the cut-off were considered in the literature: the strong ordering cut-off $\Delta = k_T/Q$ and the angular ordering cut-off $\Delta = k_T/(k_T + Q)$. We checked both choices, which in our calculation do not lead to any significant differences of the results.

The parameters m_q in Eq. (3) are the masses of the quarks. Since we are interested in the low Q^2 region of the F_L structure function, the values of the masses are important. It should be noted that the integrals I_q defined by Eq. (2) are infrared finite even if we set $m_q = 0$. However, the non-zero values of the quark masses are necessary if formula (1) is extrapolated

¹This result affects the gluon distribution only at very small values of $x \lesssim 10^{-4}$.

down to $Q^2 = 0$, respecting the kinematic constraint $F_L \sim Q^4$. The non-zero quark masses then play the role of the infrared regulator.

We shall consider two scenarios for the quark masses. In the first scenario we set the masses equal to $m_q^2 \approx m_v^2/4$ where m_v denotes the mass of the lightest vector meson which can be viewed as a component in the photon wave function. This non-perturbative Vector Meson Dominance approach can be argued within the dipole model framework. In the latter one views the DIS process as the photon fluctuating into the $q\bar{q}$ pair, the color dipole which then scatters off the target through the exchange of gluons. This exchange can be related to the unintegrated gluon density function, $f(y, k_T^2)$. We thus assume that the expressions for the structure function F_L within photon-gluon fusion mechanism include also the virtual vector meson contributions. This motivates the choice of the quark masses to be related to the vector meson masses.

In the second scenario, we will treat the quark masses as parameters, which can be tuned to obtain the best description of the data at small Q^2 . As we shall see in more detail in Sec. 5 masses $m_q = 140$ GeV for the u, d, s quarks provide an excellent description of the experimental data from JLab at low values of Q^2 , as in the dipole model [23].

Finally, it should be mentioned, that yet another process contributes to the F_L structure function, which originates from the virtual photon-quark interactions, with the emission of a gluon, $\gamma^* + q(\bar{q}) \rightarrow q'(\bar{q}') + g$. This contribution is treated within the standard collinear approximation as in Ref. [24]. These two mechanisms will be referred to as gluon and quark contributions respectively.

4 The model for higher twist contribution

In this section we shall describe the model for the higher twist contribution to F_L at low values of Q^2 , following exactly Ref. [4]. As discussed in Sec. 2 the structure function F_L contains significant higher twist contributions in the region of small Q^2 [25–27]. Such higher twists vanish when $Q^2 \rightarrow \infty$. For example, higher twists were analyzed in the context of the dipole model, together with the saturation of the dipole cross section. It was demonstrated that this framework predicts large contributions from the higher twists to the longitudinal structure function [28–30].

The main idea of our approach [4] was to consider separately the regions of low and high transverse momenta of the quarks and the gluons in the proton. Integration over κ_T' in the integral (2) is divided into the region of low and high transverse momenta, $0 < \kappa_T'^2 < \kappa_{0T}^{\prime 2}$, and $\kappa_T'^2 > \kappa_{0T}^{\prime 2}$, respectively. Here, $\kappa_{0T}^{\prime 2}$ is an arbitrary phenomenological cut-off parameter,

chosen to be of the order of 1 GeV². We varied this parameter in the range 0.5 – 1.2 GeV², and found the sensitivity of the results less than about 10%.

The region of high transverse momenta is treated according to the expression from k_T -factorization, Eq. (2). In the low $\kappa_T'^2$ region, which is likely to be dominated by the soft physics, we use the ‘on-shell’ approximation which corresponds to setting transverse momentum of the gluon to zero. This allows to cast the Eq. (2) into the collinear form with the gluon density $zg(z, Q^2)$ which is obtained from an unintegrated gluon density f , see Ref. [4] for details. Next, we make the substitution:

$$\alpha_s zg(z, Q^2) \rightarrow A, \quad (12)$$

where A is a dimensionless parameter. This leads to the following representation of the higher twist contribution to F_L :

$$F_L^{HT} = 2A \sum_q e_q^2 \frac{Q^4}{\pi} \int_0^1 d\beta \beta^2 (1 - \beta)^2 \int_0^{\kappa_{0T}'^2} d\kappa_T'^2 \frac{\kappa_T'^2}{D_q^4}, \quad (13)$$

where the denominator D_q is given by

$$D_q = \kappa_T'^2 + \beta(1 - \beta)Q^2 + m_q^2. \quad (14)$$

The constant A in Eq. (12) can be fixed from the transverse structure function, F_T . We assume that the non-perturbative contribution to F_T also comes from the region of low values of $\kappa_T'^2$ and is controlled by the same parameter A . The term F_L^{HT} does not depend on x and thus can be interpreted as representing the contribution of soft Pomeron exchange with intercept 1.

It should be noted that F_L^{HT} given by equation (13) vanishes as $1/Q^2$ in the high Q^2 limit (modulo logarithmically varying factors). We call it therefore a ‘higher twist contribution’. Observe that this term will also respect the kinematic constraint $F_L \sim Q^4$ in the limit $Q^2 \rightarrow 0$.

In order to find the parameter A one needs to consider the transverse structure function F_T and perform the same approximations on it as above. In the on-shell case, that is when the gluon transverse momentum is small, the corresponding formula which describes the photon - gluon contribution to the structure function F_T is

$$F_T(x, Q^2) = 2 \sum_q e_q^2 \frac{Q^2}{4\pi} \alpha_s \int_0^1 d\beta \int d\kappa_T'^2 x_g g(x_g, Q^2) \times \\ \times \left[\frac{\beta^2 + (1 - \beta)^2}{2} \left(\frac{1}{D_q^2} - \frac{2\kappa_T'^2}{D_q^3} + \frac{2\kappa_T'^2 \kappa_T'^2}{D_q^4} \right) + \frac{m_q^2 \kappa_T'^2}{D_q^4} \right]. \quad (15)$$

The soft term in F_T is then obtained from this expression by integrating over the low $\kappa_T'^2$ region ($\kappa_T'^2 < \kappa_{0T}'^2$). Finally, we perform the same substitution as in Eq. (12) and we identify this soft part of F_T with the ‘background’ term F_2^{Bg} of Ref. [18], i.e.

$$F_2^{Bg} = A \times \frac{\sum_q e_q^2}{\pi} \int_0^\infty dt \int_0^{\kappa_{0T}'^2} d\kappa_T'^2 \left[\frac{1}{2} \left(\frac{1}{D_q^2} - \frac{2\kappa_T'^2}{D_q^3} + \frac{2\kappa_T'^2 \kappa_T'^2}{D_q^4} \right) + \frac{m_q^2 \kappa_T'^2}{D_q^4} \right], \quad (16)$$

where now

$$D_q = m_q^2 + \kappa_T'^2 + t. \quad (17)$$

A possible weak x dependence of F_2^{Bg} is neglected and we set $F_2^{Bg} = 0.4$, see Ref. [18].

The complete structure function F_L is represented as $F_L = F_L^{HT} + F_L^{LT}$ where F_L^{LT} is calculated from Eqs (1) and (2) and F_L^{HT} from Eq. (13).

5 Numerical results

In this section we present numerical results for the longitudinal structure function F_L and compare them with the experimental data.

The calculated F_L is shown in Figs 2 and 3 as function of Q^2 in bins of x and as function of x in bins of Q^2 , respectively. Two sets of the quark and gluon PDFs, both at the leading order accuracy, were used: the GRV94LO [31] (used previously in Ref. [4]) and CT14LO [32]. In the region of our interest, low x and low Q^2 values the results practically do not depend on that choice. We have also verified that changing from LO to NLO PDFs has negligible impact on our results in the non-perturbative region. Therefore we stick to the LO choice of the PDFs. In what follows the CT14LO parametrization² will be used.

Apart from the approach displayed in Eq. (9) we also used the unintegrated gluon density with the Sudakov form-factor, Eq. (10) and found negligible differences between these two approaches. Besides the dominant (at small x) photon-gluon fusion $\gamma^* + g \rightarrow q + \bar{q}$ mechanism, we have also included a contribution from quarks, $\gamma^* + q(\bar{q}) \rightarrow q'(\bar{q}') + g$, taking into account threshold effects, for details see Ref. [4].

In the calculations we took into account the contributions from u, d, s and c quarks of masses 0.35, 0.35, 0.5 and 1.5 GeV respectively ($m_{q,h}$ masses). For comparison lower quark masses equal to 0.14 GeV for u, d, s quarks were also employed ($m_{q,l}$). The parameter $\kappa_{0T}'^2$ was set to 0.8 GeV². This value was varied in the interval 0.5 – 1.2 GeV² which resulted in changing the F_L by at most 10%.

²The more modern distributions, e.g. CT18 do not contain the LO PDFs.

In Ref. [4] we also have performed calculations within the on-shell approximation, which corresponded to setting the gluon transverse momentum to zero in the photon-gluon amplitude, Eq. (2) and restricting the integration over k_T^2 to $k_T^2 \ll Q^2$. We found that the differences between off-shell and on-shell calculations are small, particularly in the low Q^2 region. Therefore in this update we only stick to the off-shell calculation.

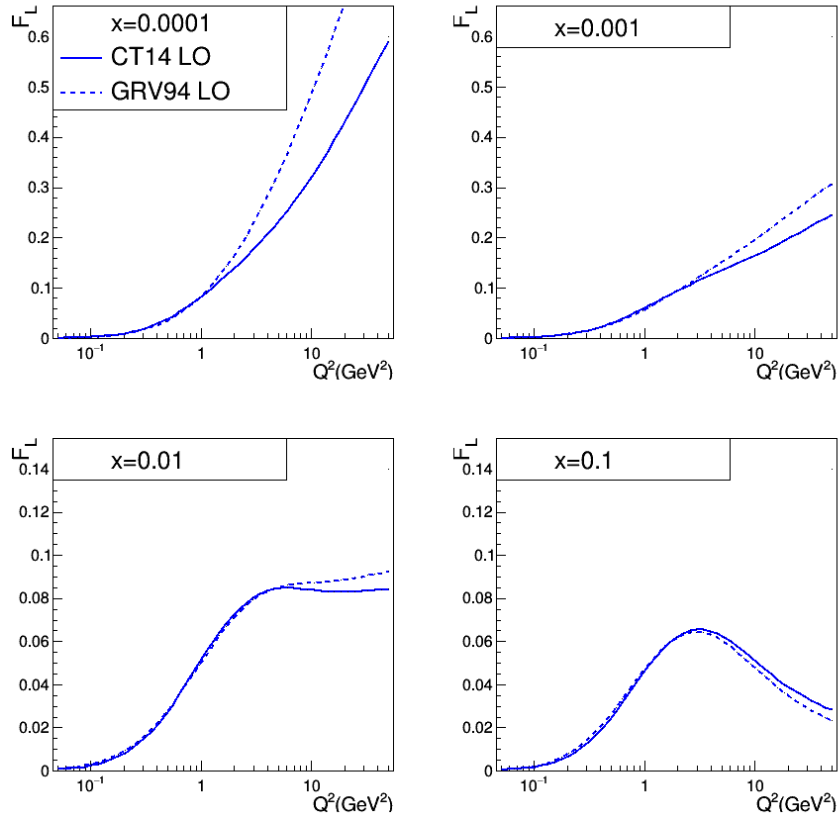


Figure 2: The results from the model for F_L for two different PDFs, CT14LO [32] and GRV94LO [31], as functions of Q^2 , in bins of x . Observe different vertical scales in upper and lower panels.

The (small) x -dependence is weak at low Q^2 and slightly growing with decreasing x while the F_L at low Q^2 and low x is very small, less than 0.005 (for $Q^2 \lesssim 0.1 \text{ GeV}^2$) and strongly decreasing with decreasing Q^2 . Contributions to F_L from the quarks, the perturbative part and the higher twist are illustrated in Figs 4 - 5 and clearly visualize the interplay of different mechanisms in building the F_L in our model. We note that the perturbative mechanism

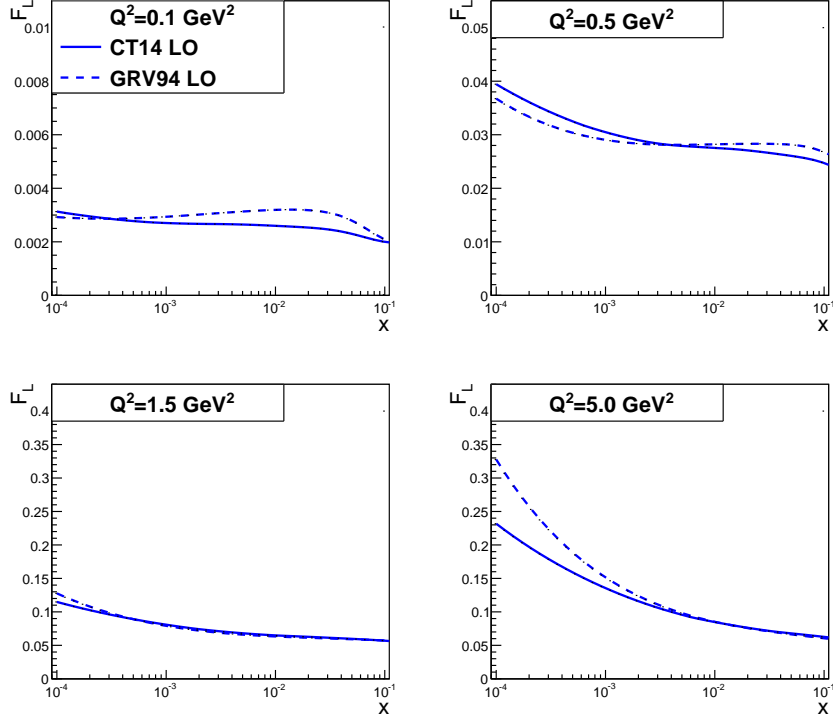


Figure 3: F_L as in Fig. 2 but as functions of x and in bins of Q^2 . Observe different vertical scales in different panels.

contributes very little in the low Q^2 region.

In Fig. 6 we compare the calculations with measurements. Unfortunately the latter are very scarce in the non-perturbative region, see Fig. 1 in Ref. [33] where a compilation of F_L measurements is given. Only results from the JLab E99-118 [34], E94-110 [35], E00-002 [33], SLAC E140X [36] and SLAC GLOBAL analysis [37] extend to the edge of the low x non-perturbative region. There our model with standard light quark masses clearly underestimates the data (broken line in Fig. 6). On the other hand, results for the set of low masses of the light quarks (u,d,s), $m_{q,l} = 0.14$ GeV which were used in the dipole model calculations [23] seem to reproduce the measurements well (continuous line in Fig. 6). The strong dependence of the results on the assumed quark masses, is illustrated in Fig. 7 for two kinematic (x, Q^2) points.

Finally, the H1 Collaboration measurements of F_L in the perturbative region at HERA, [5] are very well reproduced, see Fig. 8.

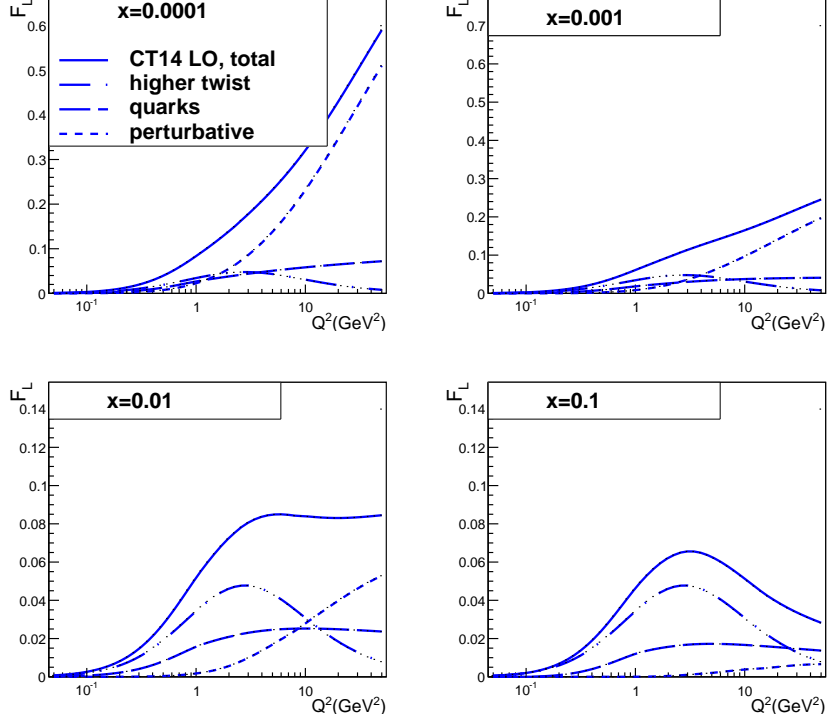


Figure 4: Contributions building the model for F_L as functions of Q^2 and in bins of x . Observe different vertical scales in the upper and lower panels.

6 Conclusions

In this paper a parametrization of the proton longitudinal structure function F_L at low Q^2 and low x is presented. It is a revisit and update of the parametrization modelled in Ref. [4] and based on the photon-gluon fusion treated in the k_T factorization, suitably extrapolated to the region of low Q^2 . There is a severe need to know F_L in this region, down to $Q^2 = 0$, in the electroproduction data analysis, e.g. in the QED radiative corrections. Unfortunately there are practically no F_L measurements in this region. This leaves the modelling constrained only at the upper end of the validity interval, as (scarce) measurements are limited to $Q^2 \gtrsim 0.1$ GeV² and $x \gtrsim 0.1$, the latter being the limit of applicability of our model.

The model fulfills the kinematic constraint $F_L \sim Q^4$ at $Q^2 \rightarrow 0$. It also contains a higher twist term, which can be interpreted as a soft Pomeron exchange. This term comes from the low transverse momenta of the quarks in the quark box diagram. The coupling of the soft

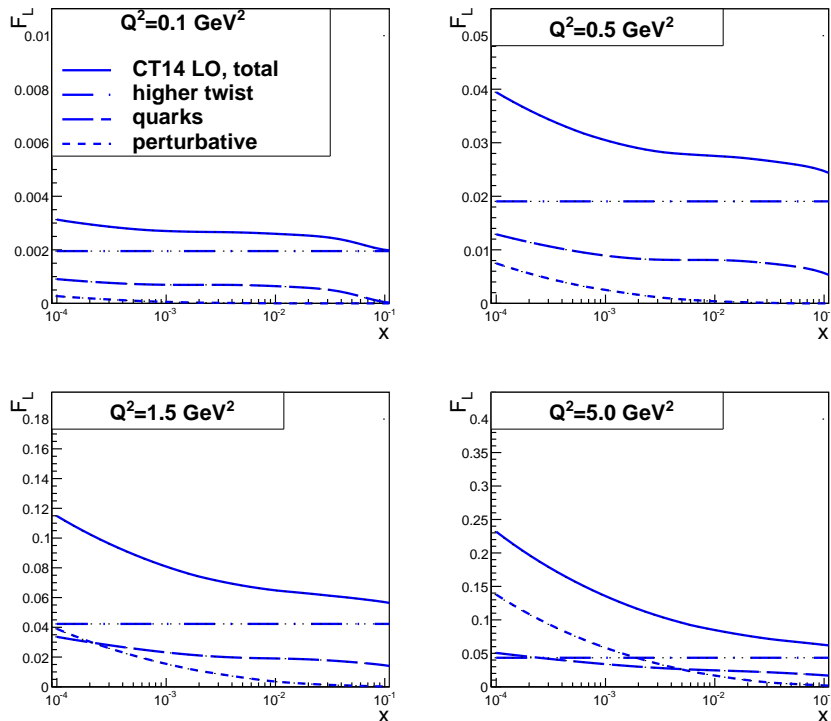


Figure 5: Contributions to F_L as in Fig. 4 but as functions of x and in bins of Q^2 . Observe different vertical scales in different panels.

Pomeron to the external virtual photon is modeled by a constant, which is fixed from the non-perturbative term of the transverse structure function. Thus our model for the higher twist in principle does not have any free parameters.

As in the previous version of the model we have used the prescription for the unintegrated gluon density as the logarithmic derivative of the standard integrated gluon density. The unintegrated gluon density which includes the Sudakov form-factor was also employed as an alternative. Compared to the old version of the model, we have used newer parton distributions. The updated parton distributions did not affect the results in the regime of low x and low Q^2 in any significant way.

The structure function F_L turns out to be very small at $Q^2 \lesssim 0.1 \text{ GeV}^2$, essentially independent of x at low x and low Q^2 and practically insensitive to the input parton distributions and perturbative accuracy (LO or NLO) of the PDFs. The model of F_L underestimates the JLab and SLAC measurements, performed at low Q^2 and $x \sim 0.1$ unless the light quark

masses are lowered down to 0.14 GeV, as in the dipole model, which brings the calculations to a very good agreement with the data. These data are however very scarce. On the other hand the model reproduces well the H1 measurements taken in the perturbative region ($Q^2 \gtrsim 1.5 \text{ GeV}^2$). In conclusion, we believe that the presented model will be useful at several stages of the data analysis, e.g. evaluation of the QED radiative corrections at the Electron Ion Collider.

Acknowledgments

We thank Fredrick Olness and Wojciech Słomiński for discussions; we express our gratitude to Eric Christy, Cynthia Keppel, Peter Monaghan, Ioana Niculescu, and Katarzyna Wichmann for supplying us with and discussing the measurements. AMS is supported by the U.S. Department of Energy grant No. DE-SC-0002145 and in part by National Science Centre in Poland, grant 2019/33/B/ST2/02588. The code for calculating $F_L(x, Q^2)$ is available upon request from the authors.

References

- [1] B. Badelek, D. Y. Bardin, K. Kurek and C. Scholz, *Z. Phys. C* **66** (1995) 591; doi:10.1007/BF01579633; arXiv:hep-ph/9403238.
- [2] COMPASS Collaboration, C. Adolph, *et al.*, *Phys. Lett. B* **753** (2016) 18; doi: 10.1016/j.physletb.2015.11.064; arXiv:hep-ex/1503.08935.
- [3] R. Abdul Khalek, *et al.*, *Science Requirements and Detector Concepts for the Electron-Ion Collider*: EIC Yellow Report, arXiv:physics.ins-det/2103.05419v3.
- [4] B. Badelek, J. Kwiecinski and A. Stasto, *Z. Phys. C* **74** (1997) 297; doi:10.1007/s002880050391; arXiv:hep-ph/9603230.
- [5] H1 Collaboration, V. Andreev *et al.*, *Eur. Phys. J. C* **74** (2014) 2814; doi:10.1140/epjc/s10052-014-2814-6; arXiv:hep-ex/1312.4821.
- [6] S. Catani, M. Ciafaloni and F. Hautmann, *Phys. Lett. B* **242** (1990) 97; doi:10.1016/0370-2693(90)91601-7.
- [7] S. Catani, M. Ciafaloni and F. Hautmann, *Nucl. Phys. B* **366** (1991) 135; doi:10.1016/0550-3213(91)90055-3.

- [8] J. C. Collins and R. K. Ellis, Nucl. Phys. B **360** (1991) 3;
doi:10.1016/0550-3213(91)90288-9.
- [9] S. Catani and F. Hautmann, Nucl. Phys. B **427** (1994) 475;
doi:10.1016/0550-3213(94)90636-X; arXiv:hep-ph/9405388.
- [10] M. Ciafaloni, Phys. Lett. B **356** (1995) 74;
doi:10.1016/0370-2693(95)00801-Q; arXiv:hep-ph/9507307.
- [11] E. M. Levin and M. G. Ryskin, Sov. J. Nucl. Phys. **53** (1991) 653;
LNF-90-025-PT.
- [12] J. Blumlein, J. Phys. G **19** (1993) 1623;
doi:10.1088/0954-3899/19/10/021.
- [13] J. Bartels, S. Gieseke and A. Kyrieleis, Phys. Rev. D **65** (2001) 014006;
doi:10.1103/PhysRevD.65.014006; arXiv:hep-ph/0107152.
- [14] J. Bartels, D. Colferai, S. Gieseke and A. Kyrieleis, Phys. Rev. D **66** (2002) 094017;
doi:10.1103/PhysRevD.66.094017; arXiv:hep-ph/0208130v2.
- [15] I. Balitsky and G. A. Chirilli, Phys. Rev. D **87** (2013) 014013;
doi:10.1103/PhysRevD.87.014013; arXiv:1207.3844 [hep-ph].
- [16] A. Bialas, H. Navelet and R. B. Peschanski, Nucl. Phys. B **593** (2001) 438;
doi:10.1016/S0550-3213(00)00640-4; arXiv:hep-ph/0009248.
- [17] A. Bialas, H. Navelet and R. B. Peschanski, Nucl. Phys. B **603** (2001) 218;
doi:10.1016/S0550-3213(01)00153-5; arXiv:hep-ph/0101179.
- [18] A. J. Askew, J. Kwiecinski, A. D. Martin and P. J. Sutton, Phys. Rev. D **47** (1993) 3775;
doi:10.1103/PhysRevD.47.3775.
- [19] K. Golec-Biernat and A. M. Stasto, Phys. Rev. D **80** (2009) 014006;
doi:10.1103/PhysRevD.80.014006; arXiv:0905.1321 [hep-ph].
- [20] M. A. Kimber, A. D. Martin and M. G. Ryskin, Eur. Phys. J. C **12** (2000) 655;
doi:10.1007/s100520000326; arXiv:hep-ph/9911379v2.

- [21] M. A. Kimber, A. D. Martin and M. G. Ryskin, Phys. Rev. D **63** (2001) 114027; doi:10.1103/PhysRevD.63.114027; arXiv:hep-ph/0101348.
- [22] K. Golec-Biernat and A. M. Stasto, Phys. Lett. B **781** (2018) 633; doi:10.1016/j.physletb.2018.04.061; arXiv:1803.06246 [hep-ph].
- [23] K. J. Golec-Biernat and M. Wusthoff, Phys. Rev. D **59** (1998) 014017; doi:10.1103/PhysRevD.59.014017; arXiv:hep-ph/9807513;
K. J. Golec-Biernat and S. Sapeta, JHEP **03** (2018) 102; doi:10.1007/JHEP03(2018)102; arXiv:1711.11360 [hep-ph].
- [24] G. Altarelli and G. Martinelli, Phys. Lett. B **76** (1978) 89; doi:10.1016/0370-2693(78)90109-0.
- [25] J. L. Miramontes, M. A. Miramontes and J. Sanchez Guillen, Phys. Rev. D **40** (1989) 2184; doi:10.1103/PhysRevD.40.2184.
- [26] J. Sanchez Guillen, *et al.*, Nucl. Phys. B **353** (1991) 337; doi:10.1016/0550-3213(91)90340-4.
- [27] S. I. Alekhin, Eur. Phys. J. C **12**(2000) 587; doi:10.1007/s100520000179; arXiv:hep-ph/9902241.
- [28] J. Bartels, K. J. Golec-Biernat and K. Peters, Eur. Phys. J. C **17** (2000) 121; doi:10.1007/s100520000429; arXiv:hep-ph/0003042v4.
- [29] J. Bartels, K. Golec-Biernat and L. Motyka, Phys. Rev. D **81** 054017 (2010) 054017; doi:10.1103/PhysRevD.81.054017; arXiv:0911.1935 [hep-ph].
- [30] L. Motyka, M. Sadzikowski, W. Słomiński and K. Wichmann, Eur. Phys. J. C **78** (2018) 80; doi:10.1140/epjc/s10052-018-5548-z; arXiv:1707.05992 [hep-ph].
- [31] M. Glück, E. Reya and A. Vogt, Z. Phys. C **67** (1995) 433; doi:10.1007/BF01624586.
- [32] A. Buckley, *et al.*, Phys. J. C **75** (2015) 132; doi:10.1140/epjc/s10052-015-3318-8; arXiv:1412.7420v2 [hep-ph].

- [33] JLab E00-002 Collaboration, V. Tvaskis, *et al.*, Phys. Rev. C **97** (2018) 045204; doi:10.1103/PhysRevC.97.045204; arXiv:1606.02614 [nucl-ex].
- [34] JLab E99-118 Collaboration, V. Tvaskis, *et al.*, Phys.Rev.Lett. **98** (2007) 142301; doi:10.1103/PhysRevLett.98.142301; arXiv:nucl-ex/0611023.
- [35] JLab E94-110 Collaboration, Y. Liang, *et al.*, arXiv:nucl-ex/0410027v2; Y. Liang, PhD thesis, The American University (2003).
- [36] SLAC E140X Collaboration, L. H. Tao *et al.*, Z. Phys. C **70** (1996) 387; doi:10.1007/s002880050117.
- [37] L. W. Whitlow, *et al.*, Phys. Lett. B **282** (1992) 475; doi:10.1016/0370-2693(92)90672-Q.

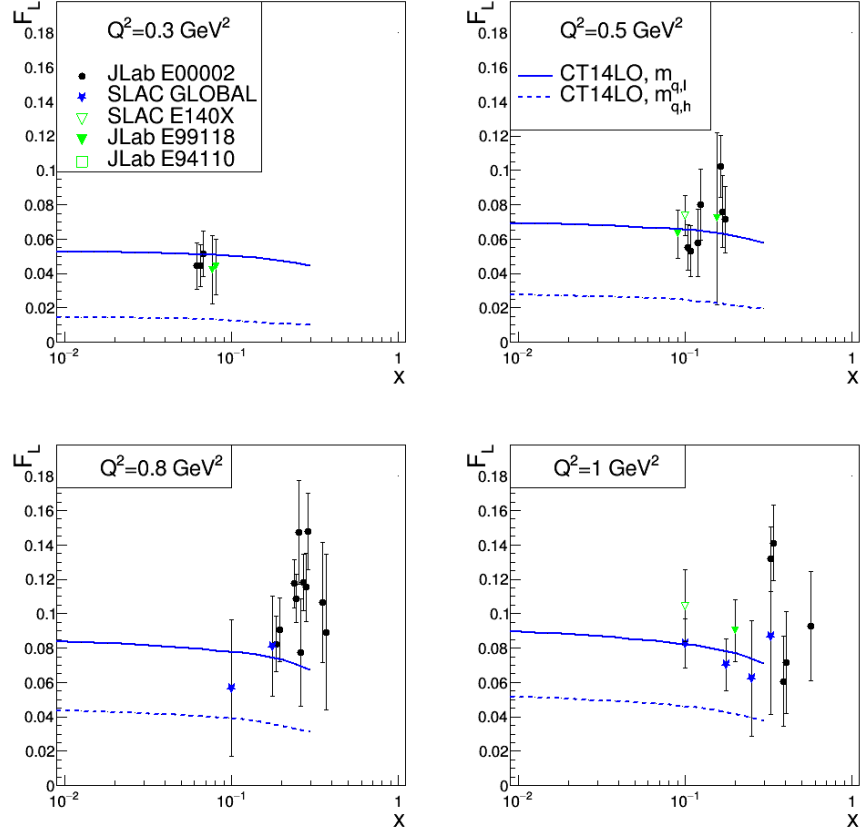


Figure 6: Model calculations for F_L for CT14LO PDFs [32], as functions of x and in bins of Q^2 , compared to the data of JLab [33–35] and SLAC [36, 37]. The broken line marks calculations performed for quark masses $m_{q,h}$ while the continuous one - for lowered light quark masses, $m_{q,l}$ according to the dipole model [23].

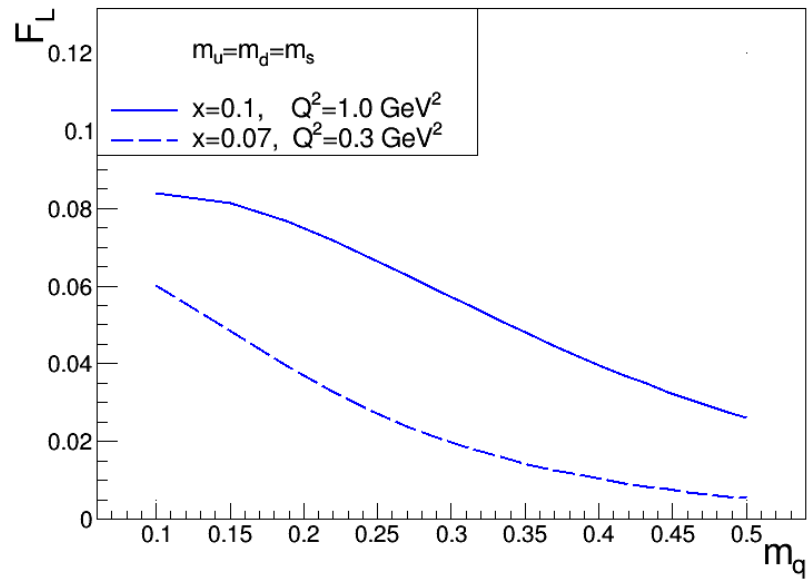


Figure 7: Results of our model calculations for F_L as function of quark masses, m_q for two pairs of the (x, Q^2) values. Equal masses of u,d,s quarks are assumed.

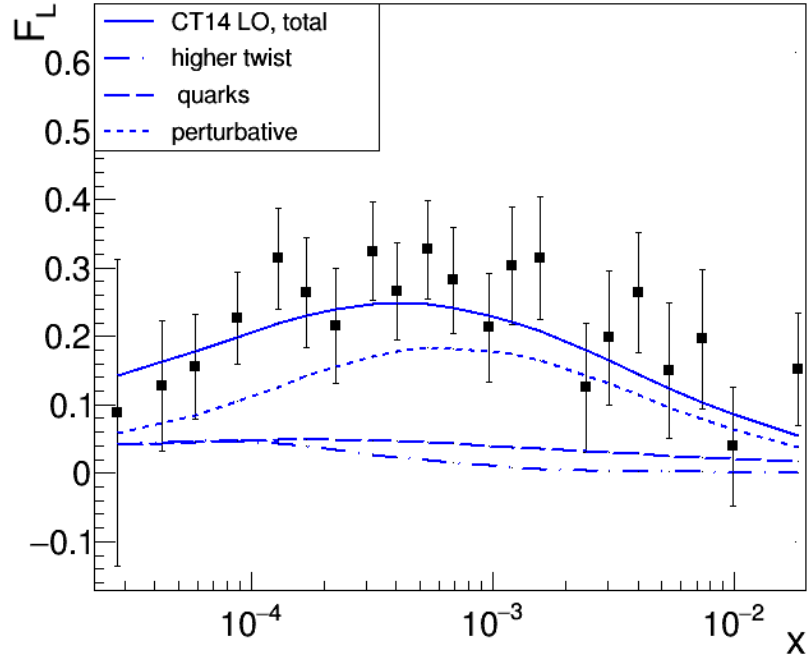


Figure 8: Results from the F_L model with CT14LO PDFs [32] compared to the HERA data from H1 experiment [5]. Each data point corresponds to a different Q^2 ; the lowest x point has lowest Q^2 equal to 1.5 GeV^2 . Contributions to the model are also marked.